# Melting of sodium clusters

Juan A. Reyes-Nava, Ignacio L. Garzón, Marcela R. Beltrán† and Karo Michaelian
*Instituto de Física, Universidad Nacional Autónoma de México*
*Apdo. Post. 20-364, México D.F., 01000 México.*
†*Instituto de Investigaciones en Materiales, Universidad Nacional Autónoma de México*
*Apdo. Post. 70-360, México D.F., 01000 México.*

Recibido el 9 de marzo de 2002; aceptado el 20 de junio de 2002

Thermal stability properties and the melting-like transition of $Na_N$, $N$ = 13-147, clusters are studied through microcanonical molecular dynamics simulations. The metallic bonding in the sodium clusters is mimicked by a many-body Gupta potential based on the second moment approximation of a tight-binding Hamiltonian. The characteristics of the solid-to-liquid transition in the sodium clusters are analyzed by calculating physical quantities like caloric curves, heat capacities, and root-mean-square bond length fluctuations using simulation times of several nanoseconds. Distinct melting mechanisms are obtained for the sodium clusters in the size range investigated. The calculated melting temperatures show an irregular variation with the cluster size, in qualitative agreement with recent experimental results. However, the calculated melting point for the $Na_{55}$ cluster is about 40 % lower than the experimental value.

*Keywords:* Metal clusters; sodium clusters; melting in clusters; phase transitions in clusters.

La fusión y las propiedades de estabilidad térmica de cúmulos de $Na_N$, $N$ = 13-147, se estudian utilizando simulaciones de dinámica molecular en el ensamble microcanónico. El enlace metálico en los cúmulos de sodio se modela con un potencial de Gupta de muchos cuerpos que se basa en la aproximación de segundo momento de un hamiltoniano de amarre fuerte. Las características de la transición sólido a líquido en los cúmulos de sodio se analizan mediante el cálculo de cantidades físicas como la curva calórica, el calor específico y la desviación cuadrática media de las fluctuaciones en las distancias interatómicas, utilizando tiempos de simulación de varios nanosegundos. Mecanismos diferentes de fusión se obtuvieron para cúmulos de sodio en el rango de tamaños investigados. Las temperaturas de fusión calculadas muestran una variación irregular como función del tamaño del cúmulo, en acuerdo cualitativo con resultados experimentales recientes. Sin embargo, el punto de fusión calculado para el cúmulo de $Na_{55}$ es aproximadamente 40 % más bajo que el valor experimental.

*Descriptores:* Cúmulos metálicos; cúmulos de sodio; fusión en cúmulos; transición de fase en cúmulos.

PACS: 36.40.-c; 36.40.Mr

## 1. Introduction

The study of the thermal stability and melting transition of sodium clusters is nowadays a very active field of research. This interest is motivated, in part, by the fact that just recently it was possible to make direct comparisons between theoretical results, mainly extracted from computer simulations [1–8], and experimental data [9–12] obtained for the melting-like transition of sodium clusters of different sizes. In fact, during the last few years the caloric curve, heat capacity, and melting temperatures of $Na_N$, $N$ = 55-200, clusters have been measured using the temperature dependence of the fragmentation mass spectra [10–12]. The melting points of these clusters were found to be on average 33 % (120 K) lower than the bulk value, and more surprisingly, large variations were observed in the melting temperatures ($\pm$ 30 K) with changing cluster size [11].

On the theoretical side, molecular dynamics (MD) and Monte Carlo (MC) methods have been used to provide microscopic descriptions on the melting mechanisms of sodium clusters in the size range of 8-147 atoms. In these studies, the metallic bonding of the sodium clusters has been described using different levels of approximation, from empirical many-body model potentials [2, 5] and tight-binding hamiltonians [3, 7] to first-principles density functional theory [1, 4, 6, 8].

Despite the large amount of information obtained from the above theoretical studies, several questions on, for example, the irregular variations of the melting temperatures with respect to the cluster size remain unsolved. One difficulty existing in the theoretical approaches to study the melting-like transition of sodium clusters is related with the interplay between the geometric and electronic structure effects in such systems [5, 6, 11]. Although MD simulations that use density functional theory explicitly take into account the electronic degrees of freedom and their effects in the cluster geometry, the limitation of this approach is related to the relatively short simulation times (a few picoseconds) during which time-averages of the structural and dynamical properties are calculated. This problem, caused by the extremely large computational effort involved in the first-principles MD simulations, is especially critical in the study of the melting transition where large thermal fluctuations are present, and therefore much longer simulation times are required to calculate converged time averages.

On the other hand, MD simulations based on many-body model potentials allow extension of the simulation time up to the nanosecond regime, employing reasonable computational resources. However, in this case the description of the metallic bonding does not explicitly include the electronic degrees of freedom. In the present work, we adopt the latter approach to perform molecular dynamics simulation of the melting-

like transition of $Na_N$, $N$ = 13, 20, 55, 135, 142, and 147, clusters using a many-body Gupta potential [13–15], and simulation times of $\sim 50$ nanoseconds. The objectives of this study are: (1) to test the phenomenological many-body Gupta potential in the description of the melting transition using adequate simulation times and (2) to compare the predictions of this simulation with those obtained from the same many-body potential but using the MC method [5, 7] for the averaging procedure, and also with the results obtained from first-principles MD [6, 8] using shorter simulation times. These tests and comparisons will provide additional insights on the melting mechanisms in sodium clusters and provide useful information on the performance of the different simulation methods.

In Sec. 2 we describe the model potential and provide details on the simulation method. Results on the caloric curves, heat capacities and thermal stability properties of different cluster sizes are given in Sec. 3. A summary of this work is presented in Sec. 4.

## 2. Metallic potential and simulation procedure

The many-body model potential used in this work corresponds to the Gupta potential [13] that is based on the second moment approximation of a tight-binding hamiltonian [14]. Its analytical expression is given by

$$V = \sum_{i=1}^{N} V_i, \tag{1}$$

$$V_i = A \sum_{j \neq i} e^{-p \ \frac{r_{ij}}{r_0} - 1} \ - \xi \left( \sum_{j \neq i} e^{-2q \ \frac{r_{ij}}{r_0} - 1} \right)^{\frac{1}{2}}, \tag{2}$$

where $r_0$, $A$, $\xi$, $p$, and $q$ are adjustable parameters [14]. For sodium clusters these parameters have been fitted to band structure calculations [15]. Their values are: $A = 0.01595$ eV, $\xi = 0.29113$ eV, $r_0 = 6.99$ bohr, $p = 10.13$, and $q = 1.30$ [15]. This type of potential has been extensively utilized in other metal cluster simulations [16–20], obtaining good agreement with results generated from first-principles methods.

In order to study the cluster melting-like transition, we use the constant-energy MD method to calculate the structural changes as a function of the cluster energy. Within this method, Newton's equations of motion are solved for each atom within the cluster using the Verlet algorithm [21]. Through this procedure, one obtains the atomic positions and momenta as a function of time, that are used to calculate time-averages of physical quantities characterizing the cluster structure and dynamics. A typical calculation consists in heating up a cluster from its zero temperature configuration until it transforms into a liquid-like cluster. To simulate this procedure the cluster total energy is increased in a step-like manner by scaling up the atomic velocities and therefore augmenting the kinetic energy of the cluster.

The simulation starts by slightly perturbing the coordinates corresponding to the lowest-energy configuration of the cluster and setting up the atomic momenta to a zero value, in order to eliminate the translation of the cluster center of mass and its rotational motion. The time step of the MD runs is 2.4 fs, which provides total energy conservation within 0.001 %. For each initial condition the cluster is equilibrated during $10^4$ time steps and the time averages are calculated using $10^7$ time steps in the solid and liquid regions, but 2 times longer simulation times are used in the melting-like transition region. This amount of averaging time is a necessary condition to obtain converged physical quantities characterizing the melting process in these finite systems.

To obtain the lowest-energy structure of each cluster size we combine simulated quenching techniques [17] and evolutive algorithms [22], which are able to perform global searches of the potential energy surface (PES) in a very efficient way despite the large number of degrees of freedom involved in the cluster structure optimization. These methods do not only provide the lowest-energy configuration but the distribution of isomers in the low energy range. This optimization procedure has been successfully used in other cluster structure optimizations [18–20, 22].

The behavior of the structural and thermal properties during the heating process of the cluster is monitored by calculating the temperature, heat capacity, and root-mean-square (rms) bond length fluctuations as a function of the cluster total energy using the following expressions:

$$T = \frac{2\langle E_k \rangle}{(3N-6)k_B}, \tag{3}$$

$$\frac{C}{Nk_B} = \left[ N - N\left(1 - \frac{2}{3N-6}\right)\langle E_k \rangle \langle E_k^{-1} \rangle \right]^{-1}, \tag{4}$$

$$\delta = \frac{2}{N(N-1)} \sum_{i<j}^{N} \frac{[\langle r_{ij}^2 \rangle - \langle r_{ij} \rangle^2]^{1/2}}{\langle r_{ij} \rangle}, \tag{5}$$

where $E_k$ is the cluster kinetic energy, $k_B$ is the Boltzmann constant, $\langle ... \rangle$ denotes a time average, and $r_{ij}$ corresponds to the distance between atoms $i$ and $j$. The above mathematical expressions were introduced in Refs. 23 and 24 in order to calculate structural and thermal properties of clusters from computer simulation studies.

## 3. Results and discussion

### 3.1. $Na_{13}$

The lowest-energy configuration of the $Na_{13}$ cluster corresponds to an icosahedral structure shown in Fig. 1a. This geometry was used to initiate the heating up procedure through the MD method. The cluster temperature (caloric curve) and specific heat as a function of the cluster total energy, calculated using Eqs. (3) and (4), are displayed in

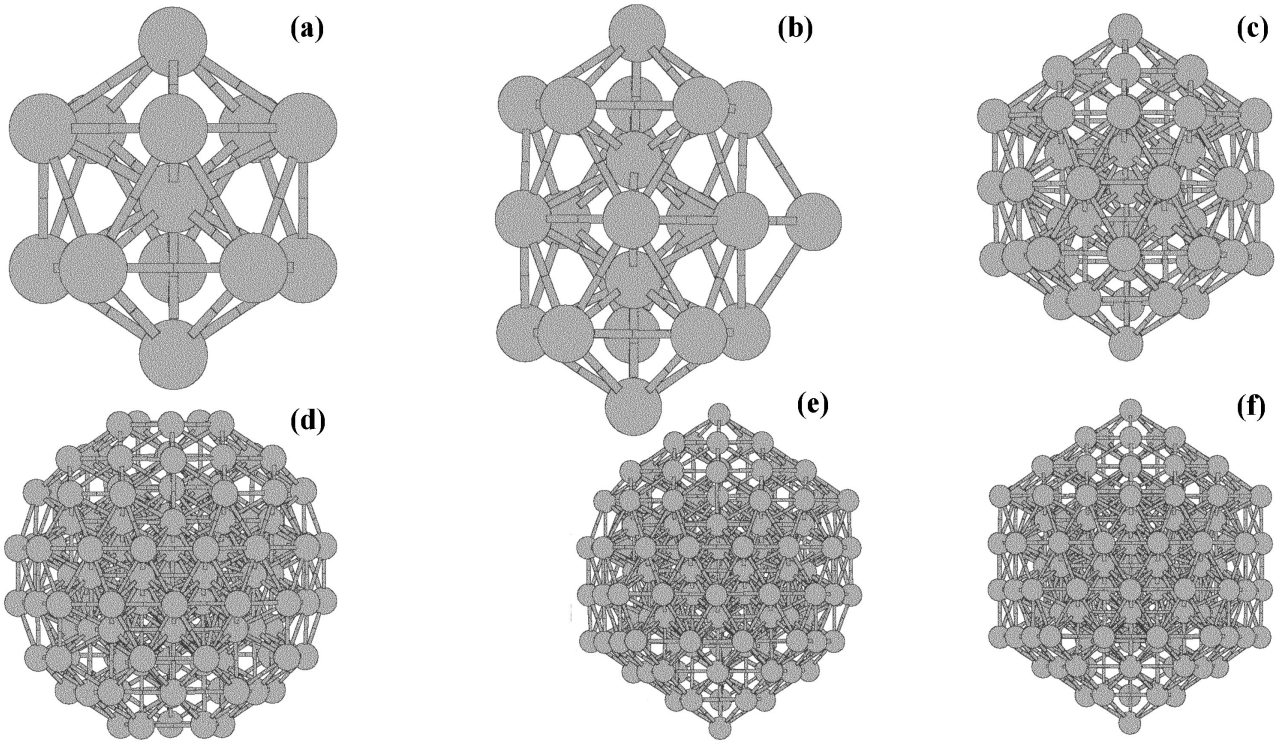


FIGURE 1. Lowest-energy structures of $Na_N$, $N$ = 13 (a); 20 (b); 55 (c); 135 (d); 142 (e); and 147 (f); clusters. The cluster geometries correspond to Mackay icosahedra for $N$ = 13, 55, and 147; a capped double icosahedron for $N$ = 20; and incomplete three-layer Mackay icosahedra for $N$ = 135 and 142.

Figs. 2a and 3a, respectively. The change in the slope of the caloric curve as well as the existence of a maximum in the specific heat are characteristics of the solid-to-liquid transition in clusters [23–25]. These features are clearly seen in Figs. 2a and 3a, indicating a melting-like transition in the $Na_{13}$ cluster. This transition, which occurs over a broad range of energy involving one or more intermediate stages (such as isomerizations, coexistence of liquidlike and solidlike phases, partial and surface melting etc.), has been widely discussed in earlier studies of atomic clusters [26]. Figure 4a shows the rms bond-length fluctuation, $\delta$, as a function of the cluster total energy, calculated using Eq. (5). It shows two abrupt variations at different energies that are in contrast with the analog of the Lindemann criterion [27] for bulk melting, where a single abrupt increase in $\delta$ is observed.

By performing thermal quenchings from configurations generated at different total energies during the MD simulation, the different melting mechanisms occurring in the $Na_{13}$ cluster can be investigated. It is found that the first abrupt change in $\delta$ at low energy (temperature) is due to cluster isomerization involving only surface atoms, whereas the second increase at higher energy (temperature) corresponds to isomerizations where the central (bulk like) atom as well as the surface atoms are involved. The onset of the surface and volume isomerizations occur at $T$=149 and 226 K, respectively, whereas the temperature corresponding to the maximum of the specific heat (which indicates the transition to the liquidlike state) is at $T$=260 K. Similar isomerization mechanisms and transition temperature values have been obtained from MC simulations of $Na_{13}$, using the same many-body model potential [7]. A similar melting behavior has also been obtained for $Ni_{13}$ and $Al_{13}$ through MD simulations using the Gupta potential [25, 28]. Nevertheless, this melting mechanism is not exclusive of metal clusters interacting by a many-body Gupta potential since both surface and volume isomerizations have also been obtained for a 13-atom cluster modeled by a pair-wise additive potential with a soft repulsive core interaction [29].

### 3.2. $Na_{20}$

The double icosahedron with a capped atom over the central pentagonal ring displayed in Fig. 1b corresponds to the lowest-energy structure of $Na_{20}$. By heating up this cluster we obtain the caloric curve and specific heat displayed in Figs. 2b and 3b, and the rms bond length fluctuation shown in Fig. 4b. In addition to the slight change in the slope of the caloric curve at low energies, the specific heat shows a shoulder at low energy (temperature), before it reaches its maximum at higher energy (temperature). A very abrupt increase in the $\delta$ value is obtained at low energy that corresponds, according to the caloric curve, to a cluster temperature of 57 K. A second abrupt increase in $\delta$ at around 157 K is also obtained after further heating of $Na_{20}$.

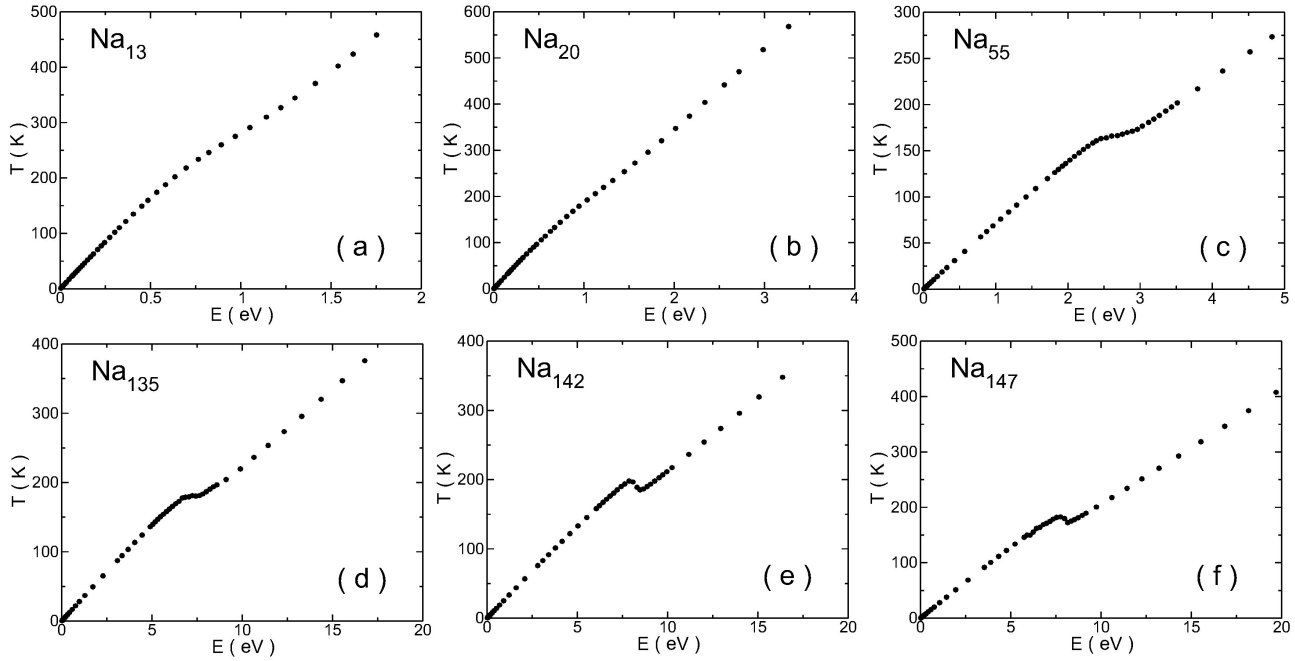


FIGURE 2. Caloric curves of $Na_N$, $N$ = 13 (a); 20 (b); 55 (c); 135 (d); 142 (e); and 147 (f); clusters. The cluster energy is calculated taking as reference the value of the binding energy of the most-stable (lowest-energy) configuration given in Table I.

The microscopic features characterizing this melting behavior can be extracted by performing periodic quenchings using the cluster configurations along the MD run at a given cluster energy. The analysis of the quenched cluster structures indicate that the first abrupt increase in $\delta$, that is in correspondence with the shoulder in the specific heat at low energies, is related with isomerization transitions where the extra atom incorporates into the cluster surface, generating a fluctuating six-atom ring in the central region of the cluster structure. This isomerization is equivalent to a surface reconstruction of the icosahedral surface without diffusion. The second jump in $\delta$ is associated to a surface melting stage where the double icosahedron transforms into a more compact structure containing two internal atoms. At higher energies (temperatures) complete melting is observed, characterized by diffusive motion where the $\delta$ value levels off. The two abrupt increases in $\delta$ obtained for $Na_{20}$ are equivalent to those described for $Na_{13}$, except that in the larger cluster the first increase corresponds to an isomerization due to the outer atom lying over the cluster surface. These phenomena occurring in $Na_{13}$ and $Na_{20}$ before they fully melt, showing atomic diffusion, can be denominated as a *premelting* stage.

The premelting phenomenon was first obtained in MD simulations of $Ni_{14}$ and $Ni_{20}$ [30–32] and some $Be_N$, $N$=9,11,12,14, clusters [33]. Later, other metal clusters with magic and non-magic number sizes also reveled a premelting stage (see, for example, Refs. 7, 25). The two-step melting transition described above was also obtained using the q-jumping MC method and the Gupta potential [5, 7]. A good agreement was found in the premelting and melting temperatures calculated with this approach [5, 7]. However, higher temperature values, for the two transitions, were found by first-principles orbital-free MD on $Na_{20}$ [6], which might be due to the much shorter simulation time used in such calculation.

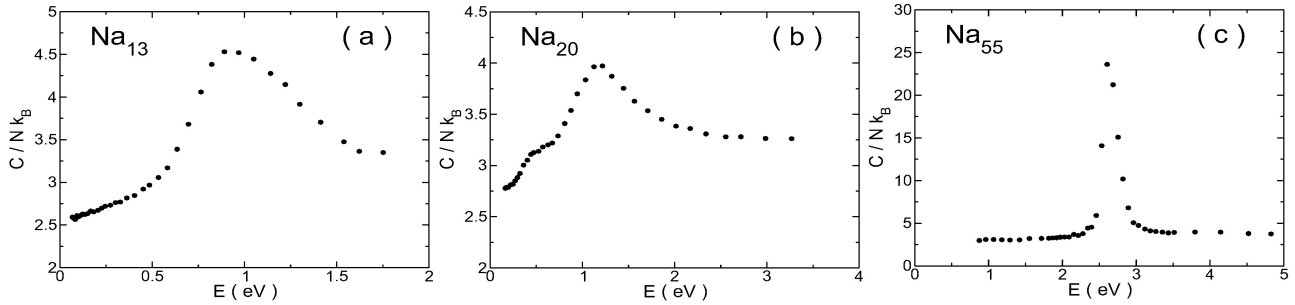


FIGURE 3. Specific heats of $Na_N$, $N$ = 13 (a); 20 (b); and 55 (c); clusters. The cluster energy is calculated taking as reference the value of the binding energy of the most-stable (lowest-energy) configuration given in Table I.

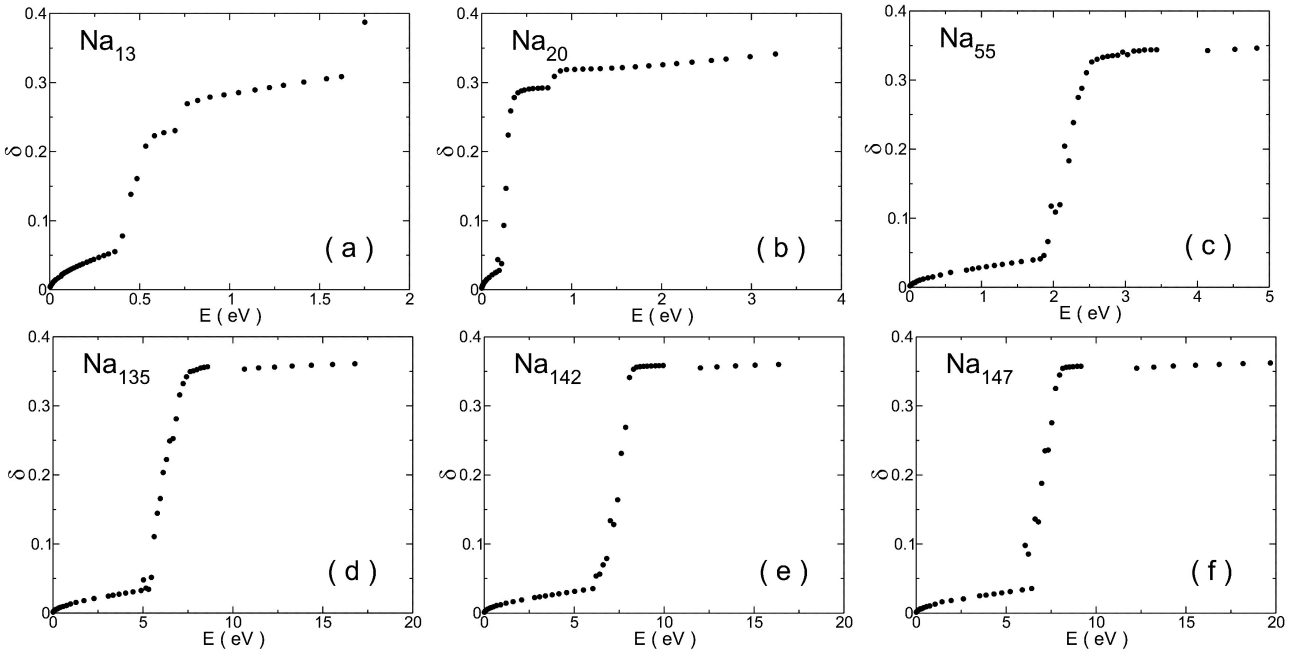


FIGURE 4. RMS bond-length fluctuations of $Na_N$, $N$ = 13 (a); 20 (b); 55 (c); 135 (d); 142 (e); and 147 (f); clusters. The cluster energy is calculated taking as reference the value of the binding energy of the most-stable (lowest-energy) configuration given in Table I.

### 3.3. $Na_{55}$

Figure 1c shows the lowest-energy configuration of $Na_{55}$ corresponding to the two-shell Mackay icosahedron. The caloric curve and specific heat obtained by heating up this structure are displayed in Figs. 2c and 3c, respectively. Figure 4c shows the rms-bond length fluctuation where an abrupt increase is observed at a total energy that, according to the caloric curve, indicates a melting temperature of 151 K, whereas the maximum in the specific heat is obtained at a slightly higher temperature of 166 K. In contrast to $Na_{13}$ and $Na_{20}$, the $Na_{55}$ cluster shows a single abrupt change in $\delta$. However, by visualizing the dynamical trajectories of each atom in the cluster at the temperatures within the transition region, we found that the melting process develops in several stages. In the first one, the most external layer fluctuates between an incomplete and complete icosahedral surface by expelling and receiving atoms back and forth. At higher energies an exchange of atoms between the intermediate and most external layers is obseved, and with a further increase in energy, fully melting is found, where the central atom also contributes to the cluster diffusive motion. This complex melting mechanism has been recently studied in $Al_{55}$ and other aluminum clusters by introducing dynamical degrees of freedom [34].

Similar melting stages have also been obtained by MC simulation of $Na_{55}$ [5, 7]. However, in those calculations a slightly higher melting temperature of 175 K was reported. The first-principles orbital-free MD simulation of $Na_{55}$ also reported [8] a melting transition at 190 K. Again, the smaller melting temperature obtained in the present work might be due to the much longer simulation times we have used in our MD simulations as compared to those used in Ref. 8. Nevertheless, none of the melting temperatures calculated by us and other authors [5, 7, 8] are in agreement with the experimental value (320 K) reported for $Na_{55}$ [12]. This discrepancy between theory and experiment has not yet been solved since it would require a more detailed modeling of the energy landscape of $Na_{55}$, that includes not only information on the basins of attraction of the equilibrium structures but also on the topology around saddle points connecting the lowest-energy minima. Additionally, in a more detailed description of the potential energy surface it would be possible that the global minimum for $Na_{55}$ does not correspond to the icosahedral structure but to an unknown special geometry with larger thermal stabiltity against melting. At present, it represents a theoretical challenge to characterize the potential energy surface of systems with such number of degrees of fredom using first-principles methods, however intense efforts are currently being performed to solve this problem. On the other hand, further experimental work is expected in the near future that confirms the relatively high value of the melting temperature of the $Na_{55}$ cluster [12].

### 3.4. $Na_{135}$, $Na_{142}$, and $Na_{147}$

The global minima of the larger sodium clusters investigated in this work correspond to icosahedral structures. The three-layer Mackay icosahedron shown in Fig. 1f, is the lowest-energy isomer of $Na_{147}$. The lowest-energy structures of the $Na_{135}$, $Na_{142}$ are incomplete icosahedra obtained by removing 12 and 5 vertex atoms, respectively, from the 147 Mackay icosahedron (see Figs. 1d and 1e, respectively). Despite the existence of an incomplete surface layer in the lowest-

energy structure of $Na_{135}$, $Na_{142}$, they show caloric curves, Figs. 2d-e, and rms bond-length fluctuations, Figs. 4d-e, very similar to those obtained by heating up the complete icosahedron structure of the 147-atom cluster, Figs. 2f and 4f. The calculated melting temperatures obtained using the Lindemann criterion ($\delta \sim 0.15$) for $Na_{135}$, $Na_{142}$, and $Na_{147}$ are 135 K, 190 K, and 171 K, respectively. These values are smaller than those obtained from the maximum of the specific heat (see Table I). By visualizing the atomic coordinates as a function of time at the energies where the $\delta$ values change abruptly, it is observed that the melting is initiated at the cluster surface. For the three sizes investigated, the atomic mobility increases with temperature starting from the most external layer and propagating into the internal layers. This stage, known as surface melting [32], precedes the complete cluster melting characterized by the diffusive motion of all the atoms in the cluster which is observed at temperatures where the specific heat is maximum.

TABLE I. Binding energies (BE) in eV/atom and melting temperatures in K calculated from the temperature value at the maximum of the specific heat and using the Lindemann criterion ($\delta \sim 0.15$). For $N$ = 13 and 20 there are two values due to the existence of two-stage (premelting and melting) transitions.

| $N$ | BE | Maximum in $C$ | Lindemann criterion | Exp.[a] |
|---|---|---|---|---|
| 13 | 0.684 | 260 | 149, 226 | |
| 20 | 0.734 | 220 | 57, 157 | |
| 55 | 0.855 | 166 | 151 | 320 |
| 135 | 0.929 | 181 | 135 | 250 |
| 142 | 0.933 | 189 | 190 | 285 |
| 147 | 0.935 | 180 | 171 | 272 |

[a]Refs. 11, 12.

Our calculated melting temperatures for these larger sodium clusters are lower than those obtained by other authors using the MC method with the same potential [5, 7] and the orbital free MD simulations [8]. This difference, as in the smaller cluster sizes, we assume is due to the much longer simulation times we have used in our MD calculations. On the other hand, although our results show that the largest melting temperature corresponds to the $Na_{142}$ cluster, in agreement with the experimental data [11, 12], the absolute values of our calculated melting temperatures are about 30 % lower than the experimental values [11, 12]. These results indicate that the many-body Gupta potential, which does not include electronic degrees of freedom, only provide a qualitative description of the melting of sodium clusters.

## 4. Summary

The melting-like transition of $Na_N$, N = 13, 20, 55, 135, 142, and 147, has been investigated through microcanonical MD simulations using a phenomenological many-body Gupta potential. The solid-to-liquid transition was studied by calculating caloric curves, rms bond-length-fluctuations and specific heats. The indicators of the cluster melting correspond to changes in the slope of the caloric curve, abrupt increases in the $\delta$ values, and the existence of maxima in the specific heats. Table I shows the melting temperatures calculated for all cluster sizes using those criteria. The main features coming out from these data are: (*i* ) The melting temperatures calculated from the maxima of the specific heats are systematically higher than the values obtained using the Lindemann criterion. (*ii* ) There is an irregular variation in the melting temperatures as a function of the cluster size, the highest value being the one corresponding to the $Na_{142}$ cluster. These results are in qualitative agreement with the experimental data [11, 12]. (*iii* ) The calculated melting temperature for the $Na_{55}$ cluster is about 40 % lower than the reported experimental value [12]. (*iv* ) The melting transition in sodium clusters is a complex phenomenon that involves several stages in which the system undergoes different structural changes (isomerization, premelting and surface melting) before it shows a diffusive regime characteristic of the liquid-like phase.

A comparison of the present results with those obtained using the same many-body potential and the MC method [5, 7], and with those generated from orbital-free MD simulations [6, 8], indicate that in general, the melting temperatures calculated by heating up the lowest-energy isomer, are lower when much longer simulation time is employed. In this work, the simulation time was extended up to the nanosecond time regime where it is very likely that the time-averages of the physical quantities that characterize the cluster melting might be much better converged.

In order to obtain a better (quantitative) agreement with the experimental results on the melting of sodium clusters it would be necessary to either extend the simulation time in the first-principles MD calculations or to design a many-body potential that describes with a higher level of approximation the complex topology of the potential energy landscape of sodium clusters. Work in both directions is currently under progress.

## Acknowledgements

This work was supported by DGSCA-UNAM Supercomputing Center. JARN acknowledges a graduate fellowship from DGEP-UNAM.

1. U. Röthlisberger and W. Andreoni, *J. Chem. Phys.* **94** (1991) 8129.
2. A. Bulgac and D. Kusnezov, *Phys. Rev. Lett.* **68** (1992) 1335.
3. R. Poteau, F. Spigelmann, and P. Labastie, *Z. Phys. D* **30** (1994) 57.
4. A. Rytkönen, H. Häkkinen, and M.Manninen, *Phys. Rev. Lett.* **80** (1998) 3940.
5. F. Calvo and F. Spiegelman, *Phys. Rev. Lett.* **82** (1999) 2270.
6. A. Aguado, J.M. López, J.A. Alonso, and M.J. Stott, *J. Chem. Phys.* **111** (1999) 6026.
7. F. Calvo and F. Spiegelman, *J. Chem. Phys.* **112** (2000) 2888; and references therein.
8. A. Aguado, J.M. López, J.A. Alonso, and M.J. Stott, *J. Phys. Chem. B* **105** (2001) 2386; and references therein.
9. T.P. Martin, *Phys. Rep.* **273** (2001) 199.
10. M. Schmidt, R. Kusche, W. Kronmüller, B. von Issendorff, and H. Haberland, *Phys. Rev. Lett.* **79** (1997) 99.
11. M. Schmidt, R. Kusche, B. von Issendorff, and H. Haberland, *Nature* **393** (1998) 238.
12. R. Kusche, T. Hippler, M. Schmidt, B. von Issendorff, and H. Haberland, *Eur. Phys. J. D* **9** (1999) 1.
13. R. P. Gupta, *Phys. Rev. B* **23** (1981) 6265.
14. V. Rosato, M. Guillope, and B. Legrand, *Philos. Mag. A.* **59** (1989) 321.
15. Y. Li, E. Blaisten-Barojas, and D.A. Papaconstantopoulos, *Phys. Rev. B* **57** (1998) 15519.
16. A. Posada-Amarillas and I.L. Garzón, *Phys. Rev. B* **54** (1996) 10362.
17. I.L. Garzón and A. Posada-Amarillas, *Phys. Rev. B* **54** (1996) 11796.
18. I.L. Garzón, K. Michaelian, M.R. Beltrán, A. Posada-Amarillas, P. Ordejón, E. Artacho, D. Sánchez-Portal, and J.M. Soler, *Phys. Rev. Lett.* **81** (1998) 1600.
19. K. Michaelian, N. Rendón, and I. L. Garzón, *Phys. Rev. B* **60** (1999) 2000.
20. K. Michaelian, M.R. Beltrán , and I. L. Garzón, *Phys. Rev. B* **65** (2002) R041403.
21. L. Verlet, *Phys. Rev.* **159** (1967) 98.
22. K. Michaelian, *Am. J. Phys.* **66** (1998) 231; *Chem. Phys. Lett.* **293** (1998) 202.
23. J. Jellinek, T.L. Beck, and R.S. Berry, *J. Chem. Phys.* **84** (1986) 2783.
24. S. Sugano, *Microcluster Physics*, (Springer-Verlag, Berlin, 1991).
25. E.B. Krissinel and J. Jellinek, in *Theory of Atomic and Molecular Clusters With a Glimpse at Experiments*, edited by J. Jellinek (Springer-Verlag, Heidelberg, 1999), pp. 277.
26. See, for example, Ref. 25, and references therein.
27. I.Z. Fisher, *Statistical Theory of Liquids*, (Univ. of Chicago Press, Chicago, 1966).
28. E.B. Krissinel and J. Jellinek, *Int. J. Quantum Chem.* **62** (1997) 185.
29. C. Rey, J. Garcia-Rodeja, L.J. Gallego, and M.J. Grimson, *Phys. Rev. E* **57** (1998) 4420.
30. J. Jellinek and I.L. Garzón, *Z. Phys. D* **20** (1991) 239.
31. I.L. Garzón and J. Jellinek, in *Physics and Chemistry of Finite Systems: From Clusters to Cristals*, Vol. 1, edited by P. Jena, S.N. Khanna, and B.K. Rao (Kluwer Academic Publishers, Dordrecht, 1992) p. 402.
32. Z.B. Güvenç and J. Jellinek, *Z. Phys. D* **26** (1993) 304.
33. C.E. Román-Velázquez and I.L. Garzón, *Z. Phys. D* **26** (1993) S134.
34. J. Jellinek and A. Goldberg, *J. Chem. Phys.* **113** (2000) 2570.